THE ANATOMICAL RECORD 296:921–932 (2013)

Novel Spatiotemporal Glycome Changes in the Murine Placenta During Placentation Based on BS-I Lectin Binding Patterns

CHRISTINA CHARALAMBOUS, KATERINA DRAKOU, STAVROS NICOLAOU, AND PANTELIS GEORGIADES*
Department of Biological Sciences, University of Cyprus, University Campus, Nicosia, Cyprus

ABSTRACT

Although spatiotemporal changes of the glycome (full set of glycans, otherwise known as saccharides or carbohydrates) during placenta formation (placentation) are functionally and clinically important, they are poorly defined. Here, we elucidated novel aspects of the glycome during mouse placentation, from embryonic day 6.5 (E6.5) to E12.5, by investigating the largely unexplored binding distribution of lectin I from *Bandeiraea simplicifolia* (BS-I lectin), a glycan-binding protein that recognizes the DGalNAc and DGal glycans found at the terminal ends of specific oligosaccharides attached to lipids or proteins. We show that BS-I lectin binding marks all trophoblast cells during early placentation (E7.5 and E8.5 stages), continues in labyrinthine and junctional zone trophoblast but is lost from parietal trophoblast giant cells by E10.5/E11.5 (definitive placenta stage) and is lost from all trophoblast types, but marks the fetal capillary endothelium of the labyrinth, by E12.5. In the decidua basalis (the maternal part of the placenta), BS-I lectin positivity mainly marks the decidual stroma cells of the venous sinusoid area (E7.5 and E8.5 stages) and the entire decidua basalis by E10.5, as well as the osteopontin-positive subset of uterine natural killer (uNK) cells from E7.5 onwards. This work provides the first comprehensive description of the hitherto ill-defined spatiotemporal binding distribution of BS-I lectin in the fetal and maternal placenta between E6.5 and E12.5, thereby contributing to glycome elucidation during placentation. It also establishes BS-I lectin positivity as a novel pan-trophoblast marker during early placentation and as a new marker for mature uNK cells from E7.5 onwards. Anat Rec, 296:921–932, 2013.

Key words: glycome; *Bandeiraea simplicifolia* lectin I; placenta; trophoblast development; uNK cells

The glycome, or complete set of glycans (sugars or saccharides), of an organ includes the glycan part of all glycoconjugates (proteins or lipids covalently attached to glycans) present in it. Although glycans are best known for their ubiquitous role in energy metabolism, they also have more specific functions during embryonic development by

*Correspondence to: Pantelis Georgiades, Department of Biological Sciences, University of Cyprus, University Campus, P.O. Box 20537, 1678 Nicosia, Cyprus. Fax: +357-22892881. E-mail: pgeor@ucy.ac.cy

Received 18 December 2012; Accepted 14 March 2013.
DOI 10.1002/ar.22698
Published online 12 April 2013 in Wiley Online Library (wileyonlinelibrary.com).

regulating cell differentiation, proliferation and signaling (Ohtsubo and Marth, 2006; Freeze and Elbein, 2009; Varki and Sharon, 2009). These specific roles are typically mediated by glycans in the form of linear or branched oligosaccharides (polymers of 2–20 monosaccharide units) covalently linked to proteins or lipids, constituting glycoproteins or glycolipids, respectively (Gabius and Wu, 2006). Glycoproteins, glycolipids, and proteoglycans [the latter being glycoprotein subtypes whose glycans are polysaccharides (i.e., polymers of more than 20 monosaccharide units)] are collectively known as glycoconjugates (Varki and Sharon, 2009) and can be cell membrane-associated, intracellular, or secreted (Laughlin and Bertozzi, 2009). Interestingly, the biological information contained within the glycome is not directly coded by the genome and is far more complex than that of the proteome. Moreover, this information modifies the function of the attached proteins/lipids and changes during development in a spatiotemporally dependent manner (Ohtsubo and Marth, 2006; Varki and Sharon, 2009).

The glycome of the placenta and that of its major cell type, the trophoblast, is not only crucial for its development but may also be clinically important. However, a complete description of placenta/trophoblast glycan profile (especially the glycan part of its glycoconjugates) and how it changes during placental formation (placentation), is unknown (Than et al., 2012). For example, inhibition of glycosylation (the enzymatic covalent addition of glycans to proteins or lipids that is a major force in mediating glycome changes) using tunicamycin (a small molecule inhibitor of glycosylation via inhibition of glycosyltransferases) resulted in trophoblast abnormalities. Specifically, addition of tunicamycin during mouse blastocyst outgrowth culture (an *in vitro* system for the study of early postimplantation trophoblast development) or in a human trophoblast cell line, resulted in defective morphological differentiation of the trophoblast and in abnormal trophoblast gene expression, respectively (Webb and Duksin, 1981; Ito and Chou, 1984). Moreover, a defective glycome has been associated with human placental pathology as shown by several studies including the detection of (a) abnormal protein glycosylation in missed abortion placentas (Šerman et al., 2004) or (b) decreased levels or loss of certain glycoconjugate-associated glycans in preeclamptic placentas (Marini et al., 2011).

Lectins are nonenzymatic, nonimmune, and nontransport glycan-binding proteins present in all organisms. They are largely responsible for decoding the glycome by binding to specific oligosaccharide glycans in glycolipids and glycoproteins (Rüdiger and Gabius, 2001; Varki et al., 2009), usually specific for one to three monosaccharides, typically situated at the outer end of the attached oligosaccharide (Varki et al., 2009). The lectin used here is one of several lectins (lectin I) from the African legume plant *Bandeiraea simplicifolia* (BS) or *Griffonia simplicifolia* (GS), abbreviated to BS-I or GS-I lectin. Its glycan binding specificity is for the monosaccharides α-linked 2-acetamido-2-deoxy-D-galactopyranose (DGalNAc) and α-linked D-galactose (DGal) found at the outer end of specific oligosaccharides within glycoconjugates (Wood et al., 1979; Lescar et al., 2002). Because plant lectins can mediate interactions between different species by binding to specific glycans on foreign glycoconjugates (Ambrosi et al., 2005), they are widely used for elucidating the glycan profile of animal tissues (Laughlin and Bertozzi, 2009). Thus, this use of lectins, such as BS-I, is expected to contribute toward the description of glycomes (and their dynamic changes), a prerequisite to understanding glycome function (Muthana et al., 2012).

The placenta is a clinically important organ, as it is necessary for fetal viability and growth, as well as for maternal wellbeing (Georgiades et al., 2002). Placentation in mice begins soon after implantation [around embryonic day 5.0 (E5.0)] and continues until approximately mid-gestation (around E10.5–E12.5) when the definitive placenta forms (Georgiades et al., 2002; Cross et al., 2006; Hu and Cross, 2010). The definitive and developing placenta can be defined as a collection of regions where maternal and zygote-derived ("fetal") cells interact to mediate fetomaternal interactions necessary for a successful pregnancy. The placenta can be divided into two main regions: the so-called "fetal placenta" and the "maternal placenta" (or decidua basalis), with the former containing mostly zygote-derived (fetal) cells and the latter consisting of mostly maternal cells (Georgiades et al., 2002; Cross et al., 2006; Hu and Cross, 2010).

The cells of the definitive fetal placenta are mainly trophoblast [term encompassing many cell types derived from the extraembryonic ectoderm (EXE) of the implanting conceptus] and allantoic fetal vasculature (derived from the allantois). Trophoblast cells of the definitive fetal placenta come from the ectoplacental cone (EPC) and chorion, both transient EXE derivatives that exist from around E5.5 up to E9.0. At around E8.5, the chorion attaches to the EPC to form the antimesometrial region of the chorionic plate (Georgiades et al., 2002; Cross et al., 2006; Hu and Cross, 2010). The regions of the definitive fetal placenta, starting from the most mesometrial and moving antimesometrially, are as follows: (a) the zone of parietal trophoblast giant (pTG) cells (or secondary trophoblast giant cells), (b) the junctional zone, which contains spongiotrophoblasts and glycogen trophoblast cells, and (c) the labyrinth zone, which contains labyrinthine trophoblast and fetal vasculature. This zone is where exchange of oxygen/nutrients and waste products takes place between circulating maternal blood (flowing through labyrinthine trophoblast-lined spaces) and fetal blood (flowing through fetal blood vessels and their capillaries, which are lined by endothelium). The chorionic plate of the labyrinth is where the large fetal blood vessels (as opposed to their capillaries), are located (Georgiades et al., 2002).

The cells of the maternal placenta are mostly decidua basalis stromal cells, maternal immune cells, maternal vasculature, and invasive trophoblast. The maternal vasculature includes the centrally located spiral arteries and the peripherally located venous sinusoids through which maternal blood comes to or moves away from the placenta, respectively (Georgiades et al., 2002). The maternal immune cells, such as the uterine natural killer (uNK) cells (Charalambous et al., 2012; Zhang et al., 2011), as well as invasive trophoblast of this region are important for correct spiral artery wall modification, an event of crucial importance for correct placental function and fetal growth/viability (Georgiades et al., 2002; Hu and Cross, 2010; Zhang et al., 2011; Charalambous et al., 2012). Interestingly, uNK cells

contain binding sites for the Dolichos Biflorus Agglutinin (DBA) lectin (Zhang et al., 2011; Charalambous et al., 2012). Invasive trophoblasts are the spiral artery trophoblast giant (SpA-TG) cells, which show endovascular invasion of the spiral arteries by E10.5, and the invasive glycogen trophoblast cells, which show interstitial invasion of the decidua basalis stroma by E12.5 (Georgiades et al., 2002; Hu and Cross, 2010). Importantly, the maturation of the stroma cells of the decidua basalis is spatio-temporally controlled, with regions closer to the fetal placenta maturing earlier than those further away from it (Stewart and Peel, 1979). Mesometrial to the decidua basalis is the mesometrial triangle, which apparently is not invaded by invasive trophoblasts (Ain et al., 2003; Elia et al., 2011).

Our main objective was to characterize the largely unexplored spatiotemporal distribution of BS-I lectin binding in the fetal and maternal placenta during mouse placentation, between E6.5 and E12.5, thereby contributing to the elucidation of the placental glycome (and its changes) during this period.

BS-I binding is traditionally used as an endothelium marker in the vasculature of many somatic adult tissues (Laitinen, 1987) and was reported to specifically mark the fetal capillary endothelium of placental labyrinthine during late gestation (E15.5; Detmar et al., 2008). Regarding the developing fetal placenta, previous work showed that BS-I binding was undetectable in the preimplantation and E5.5 conceptus (Wu et al., 1983; Tam et al., 1993) but evident at E6.5 and E7.5 in the EPC and pTG cells (Wu et al., 1983; Azuma et al., 1991; Tam et al., 1993). However, investigation of BS-I binding in the chorion at E7.5 and in most other fetal placental trophoblast types during later stages of placentation (e.g., chorionic plate, labyrinthine trophoblast, spongiotrophoblasts and trophoblast glycogen cells), has not been done. Similarly, BS-I positivity in the decidua basalis and its associated uterus during placentation is largely unexplored. For example, it is unknown whether during this period BS-I binds to the decidua basalis stroma cells, the spiral arteries and venous sinusoids, the uNK cells, or the invasive glycogen trophoblast and SpA-TG cells. This study therefore addressed all these issues.

MATERIALS AND METHODS

Mice and Tissue Collection

ICR mice were maintained under standard conditions and noon of copulation plug day was designated E0.5. Six pregnant females were used, each producing a litter for each of the six stages examined (E6.5, E7.5, E8.5, E10.5, E11.5, and E12.5). For stages E6.5–E10.5, the entire uterine swellings were isolated including the mesometrial triangle, the myometrium, and the embryo whereas for the E11.5 and E12.5 stages the embryo was removed. These were then fixed in 4% paraformaldehyde, dehydrated and embedded in paraffin wax using standard protocols.

Sectioning and Histology

Paraffin blocks (three from each stage) were sectioned (7 μm thickness) so that the plane of sectioning was perpendicular to either the antimesometrial base of the EPC (for E6.5–E8.5) or the flat (allantoic) surface of the fetal placenta (for E10.5–E12.5). Sections were mounted on slides and stained with Hematoxylin and Eosin (H/E), using standard procedures. The sections used were central: For E6.5–E8.5, those with the largest EPC area and presence of uterine lumen remnant mesometrial to it were used, and for E10.5–E12.5, those with the largest fetal placenta area.

Chromogenic Lectin Histochemistry and Immunohistochemistry

Lectin histochemistry was carried out as reported previously (Paffaro et al., 2003). The lectins used were biotin-conjugated BS-I lectin (1:400 dilution of 1 mg/mL stock; Sigma, L3759) and biotin-conjugated DBA lectin (1:100 dilution of 1 mg/mL stock; Sigma, L6533). Immunohistochemistry was carried out as described before (Elia et al., 2011). The primary antibodies used were rabbit anti-cytokeratin (1/1000 dilution; Dako, Z0622) and rabbit anti-a-smooth muscle actin (ASMA; 1:50 dilution; Abcam, ab5694) and were detected with a goat anti-rabbit biotin-conjugated secondary antibody (Abcam, ab97073). For both lectins and antibodies, signal was achieved by incubation with streptavidin-conjugated peroxidase (Abcam, aab64269), followed by DAB chromogen reaction (Abcam), according to the manufacturer. Sections were counterstained with Hematoxylin. No specific color reaction was seen in negative control experiments (same procedure without the primary antibody or the lectin) (data not shown).

Double Fluorescent Lectin Histochemistry and Immunohistochemistry

The procedure used was the same as that previously reported for double fluorescent immunohistochemistry using two antibodies, but here one of the antibodies was replaced with the lectin (Elia et al., 2011). Briefly, paraffin sections were simultaneously incubated with biotin-conjugated BS-I lectin (1:1000 dilution of 1 mg/mL stock; Sigma, L3759) and rabbit anti-osteopontin (1:900 dilution; Abcam, ab91655). Lectin and antibody binding were detected using a streptavidin-conjugated Alexa Fluor 488 (1:500 dilution; Invitrogen, S-11223) and an anti-rabbit Cy3-conjugated secondary antibody (1:100 dilution; Abcam, ab6939), respectively. The sections were counterstained with the fluorescent nuclear marker Hoechst. The signals were visualized under fluorescent microscopy using GFP (for Alexa Fluor 488), RFP (for Cy3) and CFP (for Hoechst) filters. Negative control experiments (same procedure, but with the omission of either the primary antibody or the lectin) did not show any Cy3 or Alexa Fluor 488 signal, respectively (data not shown).

Quantification of BS-I Lectin Signal Intensity

To quantify the intensity of BS-I lectin binding strength (based on the strength of the chromogenic signal), we took advantage of the fact that all chromogenic BS-I lectin staining experiments were carried out at the same time with the duration of the chromogenic reaction being the same for all stages. Measurements were carried out on sections from at least two different implantation sites/

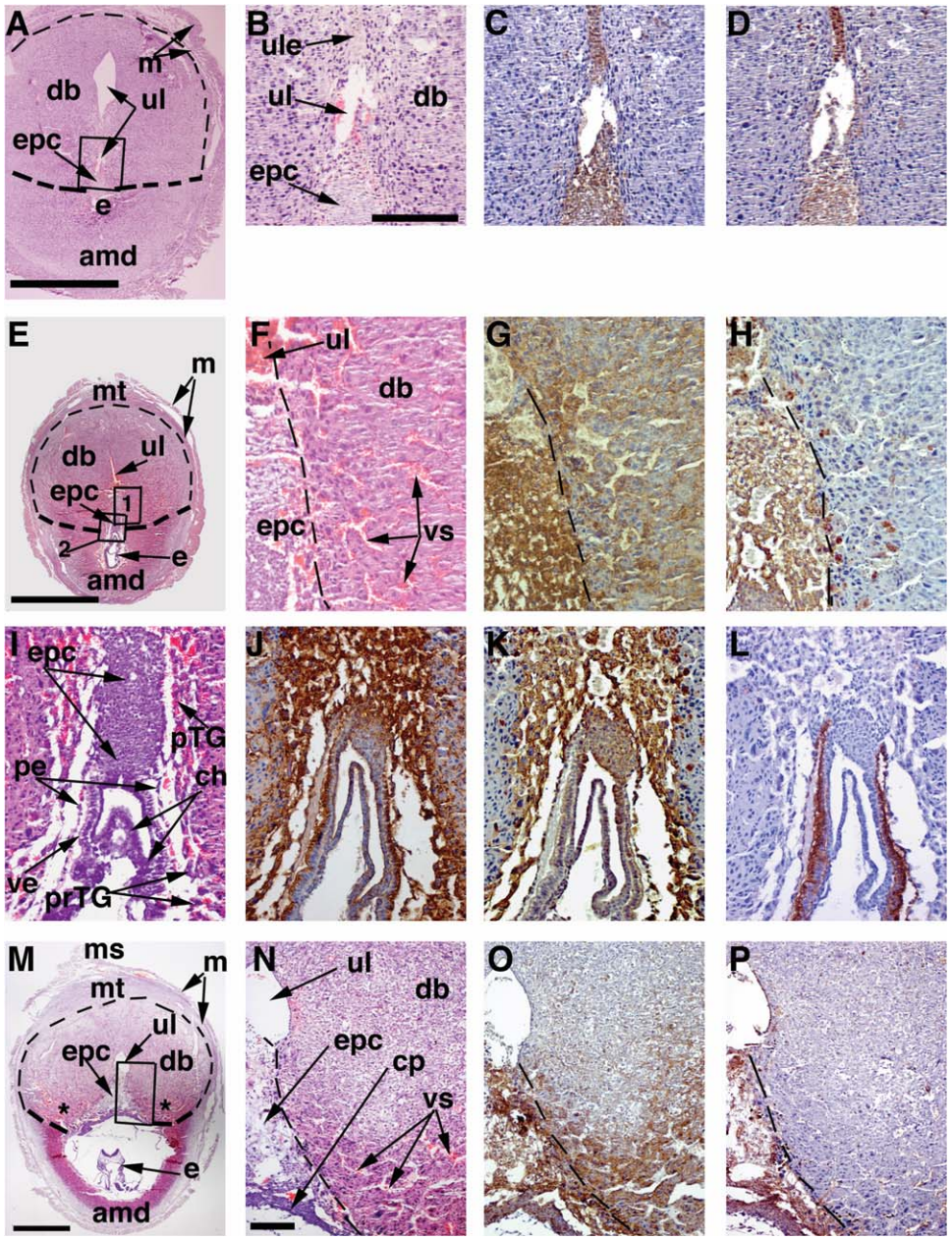

Fig. 1. Adjacent sections of the developing fetal placenta and decidua basalis at E6.5 (**A–D**), E7.5 (**E–L**), and E8.5 (**M–P**), stained with H/E (**A, B, E, F, I, M, N**), BS-I lectin (**C, G, J, O**), anti-cytokeratin antibody (**D, H, K, P**), and DBA lectin (**L**). In all images, the mesometrial pole is at the top of each panel. Panels A, E, and M are low magnification views at E6.5, E7.5, and E8.5, respectively. Panels B–D are high magnification views of the area depicted by a rectangle in A. Panels F–H and I–L are high magnifications of the area enclosed by rectangles 1 and 2 of panel E, respectively. Panels N–P are high magnifications of the area enclosed by the rectangle in M. Asterisks in M denote the venous sinusoid area (vs), which contains highly eosinophilic decidua stroma cells unlike the rest of the decidua basalis (F, N). Scale bars in A and E are 1 mm. Panels B–D and F–L are of the same magnification; scale bar in B is 400 μm. Panels N–P are of the same magnification; scale bar in N is 400 μm. Amd: antimesometrial decidua; ch: chorion; cp: chorionic plate; db: decidua basalis; e: embryo; epc: ectoplacental cone; m: myometrium; mt: mesometrial triangle; ms: mesometrium; pe: parietal endoderm; prTG: primary trophoblast giant cells; pTG: parietal trophoblast giant cells; ul: uterine lumen remnant; ule: uterine lumen epithelium; ve: visceral endoderm; vs: venous sinusoids

placentas per stage. The method employed here was described previously (Tolivia et al., 2006). Briefly, after same-magnification images were obtained, they were first processed using Adobe Photoshop software to separate the BS-I chromogenic signal from the rest of the colors in each image and to convert it into a gray-scale signal, as done before (Tolivia et al., 2006). As a result, different BS-1 signal strengths appeared as different gray intensities, whilst areas lacking BS-I positivity appeared as white areas (data not shown). Subsequently, the ImageJ

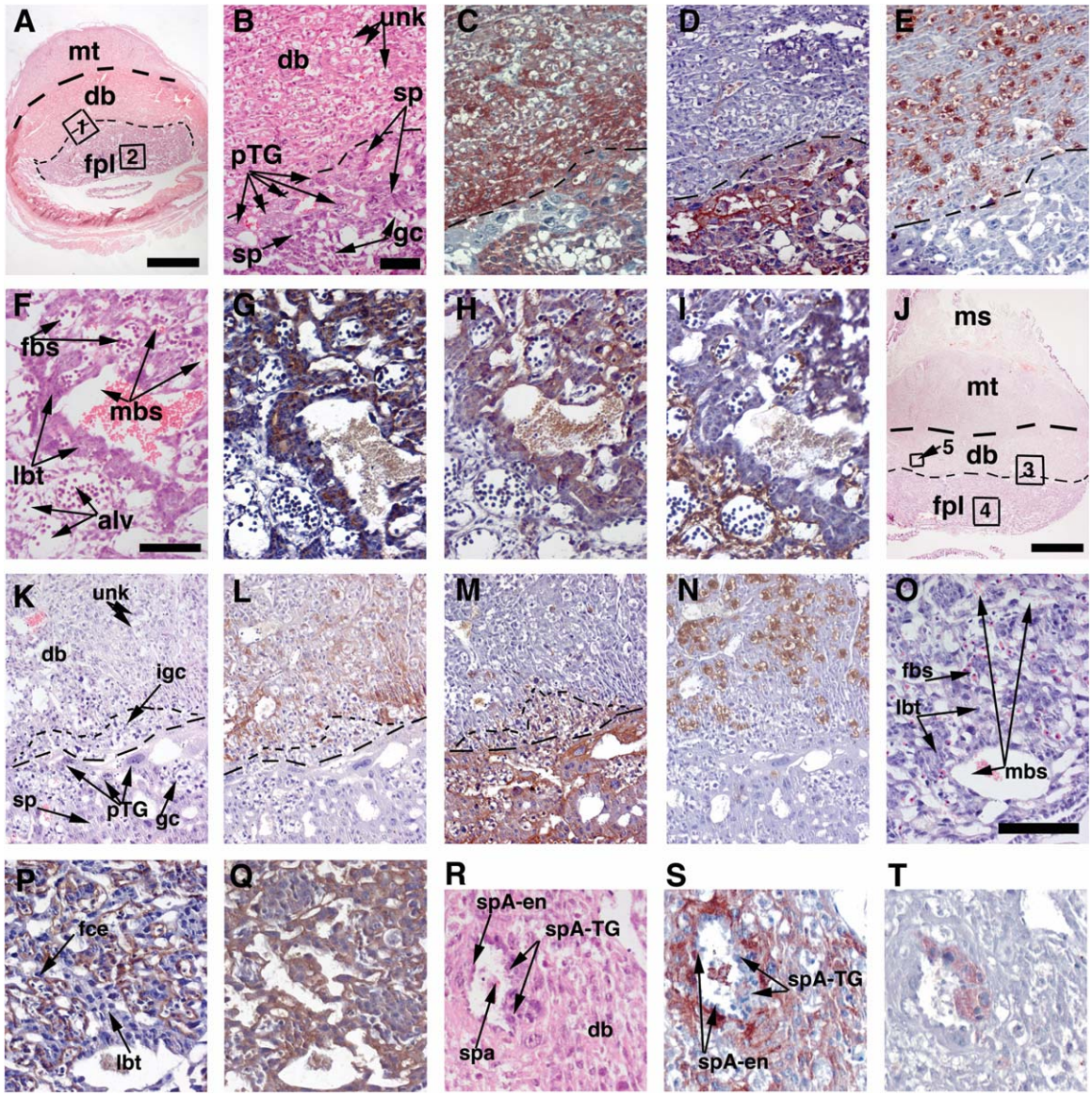

Fig. 2. Adjacent sections of the fetal placenta and decidua basalis at E10.5 (**A–I**) and E12.5 (**J–T**), stained with H/E (**A, B, F, J, K, O, R**), BS-I lectin (**C, G, L, P, S**), anti-cytokeratin antibody (**D, H, M, Q, T**), DBA lectin (**E, N**), and anti-ASMA antibody (**I**). In all images, the mesometrial pole is at the top. Panels B–F and F–I are high magnification views of the areas depicted by rectangles 1 and 2 in A, respectively. Panels K–N, O–Q, and R–T are high magnification views of the areas depicted by rectangles 3, 4, and 5 in J, respectively. Scale bars in A and J are 1 mm. Panels B–E and K–N are of the same magnification; scale bar in B is 100 μm. Panels F–I are of the same magnification; scale bar in F is 100 mm. Panels O–T are of the same magnification; scale bar in O is 100 μm. Alv: allantoic vasculature of the chorionic plate; db: decidua basalis; fpl: fetal placenta; fbs: fetal blood spaces of the labyrinth; fce: fetal capillary endothelium of the labyrinth; gc: glycogen trophoblast cells; igc: invasive glycogen trophoblast cells; lbt: labyrinthine trophoblast; m: myometrium; mbs: maternal blood spaces of the labyrinth; mt: mesometrial triangle; ms: mesometrium; mt: mesometrial triangle; pTG: parietal trophoblast giant cells; sp: spongiotrophoblast; spa: spiral artery; spA-en: spiral artery endothelium; spA-TG: spiral artery trophoblast giant cells; unk: uterine natural killer cells

freeware was used as described before (Tolivia et al., 2006) to quantify the strength of the gray signal by measuring the "mean gray value" (sum of "grayness strength" of all the pixels within the selected area divided by the total number of gray pixels within this area), with white areas having a zero value and black areas (if any) having a value of one. These measurements were done on many randomly chosen areas within the different placental compartments. Statistically, significant differences in BS-I reactivity strength (mean gray values) between the different placental areas per stage were assessed using the one-way ANOVA test. Statistically significant differences ($P < 0.05$) between grouped measurements from different placental regions per stage were considered those whose mean value did not fall within the "95% confidence interval for Mean" of other regions. Statistical significance for a given placental region across different stages was assessed between any two stages using the two-tailed unpaired t-Test

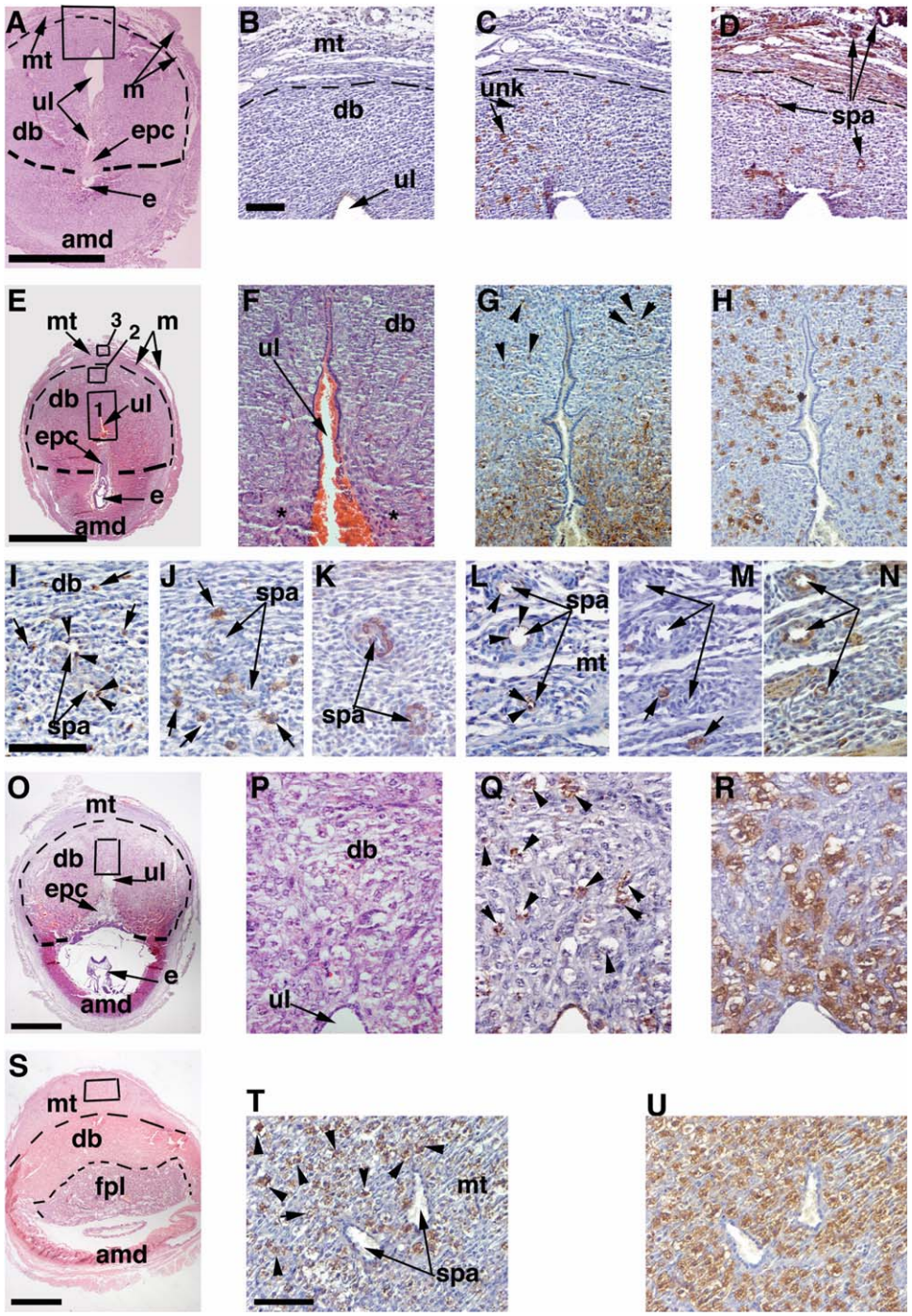

Fig. 3. Adjacent sections of the fetal placenta and decidua basalis at E6.5 (**A–D**), E7.5 (**E–N**), E8.5 (**O–R**), and E10.5 (**S–U**), stained with H/E (**A, E, F, O, P, S**), BS-I lectin (**B, G, I, L, Q, T**), DBA lectin (**C, H, J, M, R, U**), and anti-ASMA antibody (**D, K, N**). In all images, the mesometrial pole is at the top. Panels B–D are high magnification views of the area depicted by the rectangle in A. Panels F–H, I–K, and L–N are high magnification views of the areas depicted by rectangles 1, 2, and 3 in E, respectively. Panels P–R and T–U are high magnification views of the areas depicted by the rectangles in O and S, respectively. Note that E7.5, but not at E6.5, BS-I lectin binds to some endothelial cells of spiral arteries of the decidua basalis and mesometrial triangle (arrowheads in I and L) and to vacuolated cells in the decidua basalis (arrowheads in G and small arrows in I), most probably uNK cells. This putative BS-I binding to uNK cells is also seen at E8.5 (arrowheads in Q) and E10.5 (arrowheads in T). Also, note that the decidua basalis positivity for BS-I at E7.5 is confined to stoma cells that are more eosinophilic than those of the rest of the decidua (F, G). Scale bars in A, E, O, and S are 1 mm. Panels B–D and F–H are of the same magnification; scale bar in B is 100 μm. Panels I–N and P–R are of the same magnification; scale bar in F is 100 μm. Panels T and U are of the same magnification; scale bar in O is 100 μm. Amd: antimesometrial decidua; db: decidua basalis; e: embryo; epc: ectoplacental cone; fpl: fetal placenta; m: myometrium; mt: mesometrial triangle; ms: mesometrium; mt: mesometrial triangle; spa: spiral artery; unk: ul, uterine lumen remnant; uterine natural killer cells

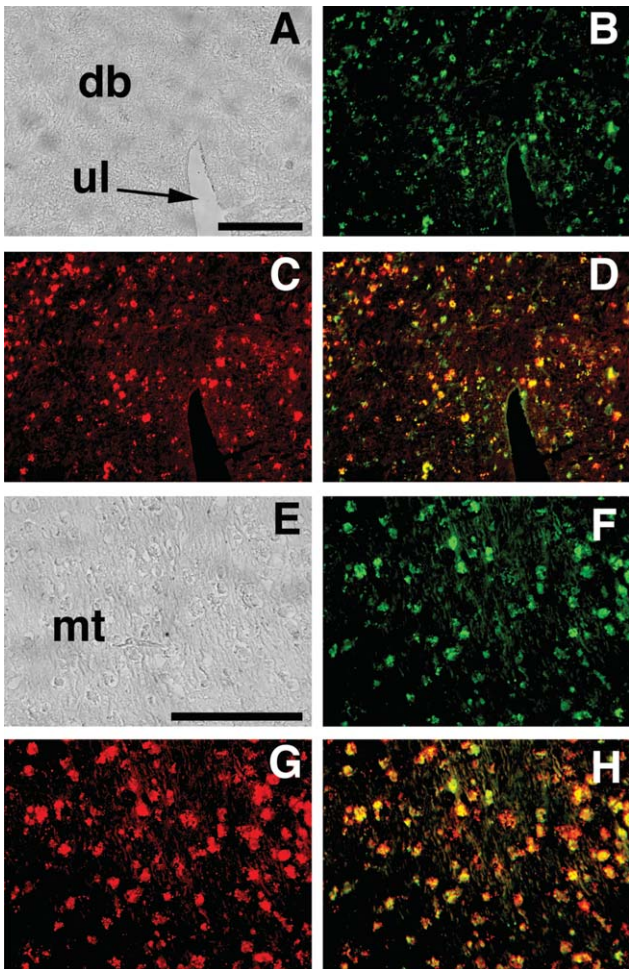

Fig. 4. Sections of E8.5 decidua basalis (**A–D**) and E12.5 mesometrial triangle (**E–H**), subjected to double immunofluorescent histochemistry with BS-I lectin (**B** and **F**, green fluorescence) and an anti-osteopontin antibody (**C** and **G**, red fluorescence), a marker of a subset of uNK cells. Panels B and C are different fluorescent views of the same section, as are panels F and G. Panels A and E are bright-field views of B/C and F/G, respectively. Panels D and H are superimpositions of B/C and F/G, respectively. Note that the overlap (yellow, yellow-green or orange signal in D and H) between BS-I signal (green spots in B and F) and osteopontin-positive uNK cells (red spots in C and G) is almost, if not entirely, complete (D and H). Panels A-D are of the same magnification; scale bar in A is 50 μm. Panels E–H are of the same magnification; scale bar in A is 50 μm. Db: decidua basalis; mt: mesometrial triangle; ul: uterine lumen remnant

(statistically significant differences were those with a P value of less than 0.05).

RESULTS

To examine the spatiotemporal distribution of BS-I binding in the developing placenta (both fetal and maternal parts) and its associated uterus during placentation, uterine sections of implantation sites from stages E6.5, E7.5, E8.5, E10.5, E11.5, and E12.5 were subjected to BS-I lectin histochemistry. In addition, adjacent sections were used in the following procedures: (a) Hematoxylin and Eosin (H/E) for general histology. (b) DBA lectin histochemistry for identifying uNK cells, visceral endoderm and parietal endoderm (Tam et al., 1993; Herington and Bany, 2007; Zhang et al., 2011). (c) Immunohistochemistry with an antibody against cytokeratin, a marker of trophoblast cells, the epithelium of uterine lumen and uterine glands and the perimetrium (outermost layer of the uterus; Charalambous et al., 2012). (d) Staining with an antibody against α-smooth muscle actin (ASMA) for identifying pericytes of the spiral arteries and mature labyrinthine fetal vessels, as well as myometrial smooth muscle (Georgiades et al., 2002; Elia et al., 2011).

Based on histology and comparison of adjacent sections stained with BS-I lectin and anti-cytokeratin antibody, a dynamic trophoblast pattern of BS-I positivity was found. Specifically, during the E6.5–E7.5 period binding of BS-I lectin was found in the EPC, pTG cells (Fig. 1C,G,J and data not shown), and primary trophoblast giant cells (nonplacental trophoblast derived from mural trophectoderm; Figs. 1J, 7F and data not shown). BS-I positivity was also detected in chorionic trophoblast at E7.5 (Fig. 1J) and its E8.5 derivative, the chorionic plate, as well as in the E8.5 EPC (Fig. 1O). At E10.5 and E11.5, BS-I binding marked the labyrinthine trophoblast, spongiotrophoblast and trophoblast glycogen cells of the junctional zone. BS-I positivity in trophoblast giant cells was undetectable from E10.5 onwards in pTG cells (Figs. 2C,G, 7I) and primary trophoblast giant cells (data not shown). Between E11.5 and E12.5, BS-I reactivity was also lost from labyrinthine and junctional zone trophoblasts. Therefore, the entire trophoblast compartment of the fetal placenta became BS-I negative by E12.5 (Fig. 2L,P). The fetal capillary endothelium of the labyrinthine was BS-I positive at both E10.5 and E12.5 (Fig. 2G,P). Interestingly, the ASMA-positive pericyte-associated mature fetal vessels of the labyrinthine chorionic plate were negative for BS-I reactivity (Figs. 2G,I, 6C,F,I,L).

Within the maternal placenta, trophoblast cells (i.e., invasive glycogen trophoblast and SpA-TG cells) are normally present in this region by E12.5, as confirmed by cytokeratin positivity in the decidua basalis. We failed to detect any BS-I lectin reactivity in these cells at E12.5 (Fig. 2L,S). Although BS-I lectin binding in the decidua basalis between E6.5 and E12.5 has not been investigated, we show here that it is detectable and dynamic. Specifically, at E6.5 BS-I positivity was confined to the epithelium of the uterine lumen remnant mesometrial to the EPC, but absent from all other cell types including stromal cells, vasculature and uNK cells (Figs. 1C, 3B, 5C). At E7.5 and E8.5 however, BS-I lectin binding was detected in the decidual stroma cells, in an area adjacent to the EPC that encompasses the venous sinusoids (Figs. 1G,O, 3G, 5I,O) that is more eosinophilic than other decidual stroma areas (Figs. 1N, 3F, 5H,N). At E7.5, but not at E8.5 or later, BS-I lectin binding was detected in some endothelia of spiral arteries (identified by their ASMA-positive pericytes and muscular walls; Elia et al., 2011; Figs. 2S, 3I,K and data not shown). BS-I lectin positivity in the decidua basalis stroma cells persists throughout the E10.5–E12.5 period, but is absent from those of the mesometrial triangle (Figs. 2C,L 6C,I). Regarding uNK cells, BS-I lectin binding was found in a subset of these cells from E7.5 onwards, as determined by comparison with adjacent sections stained with the

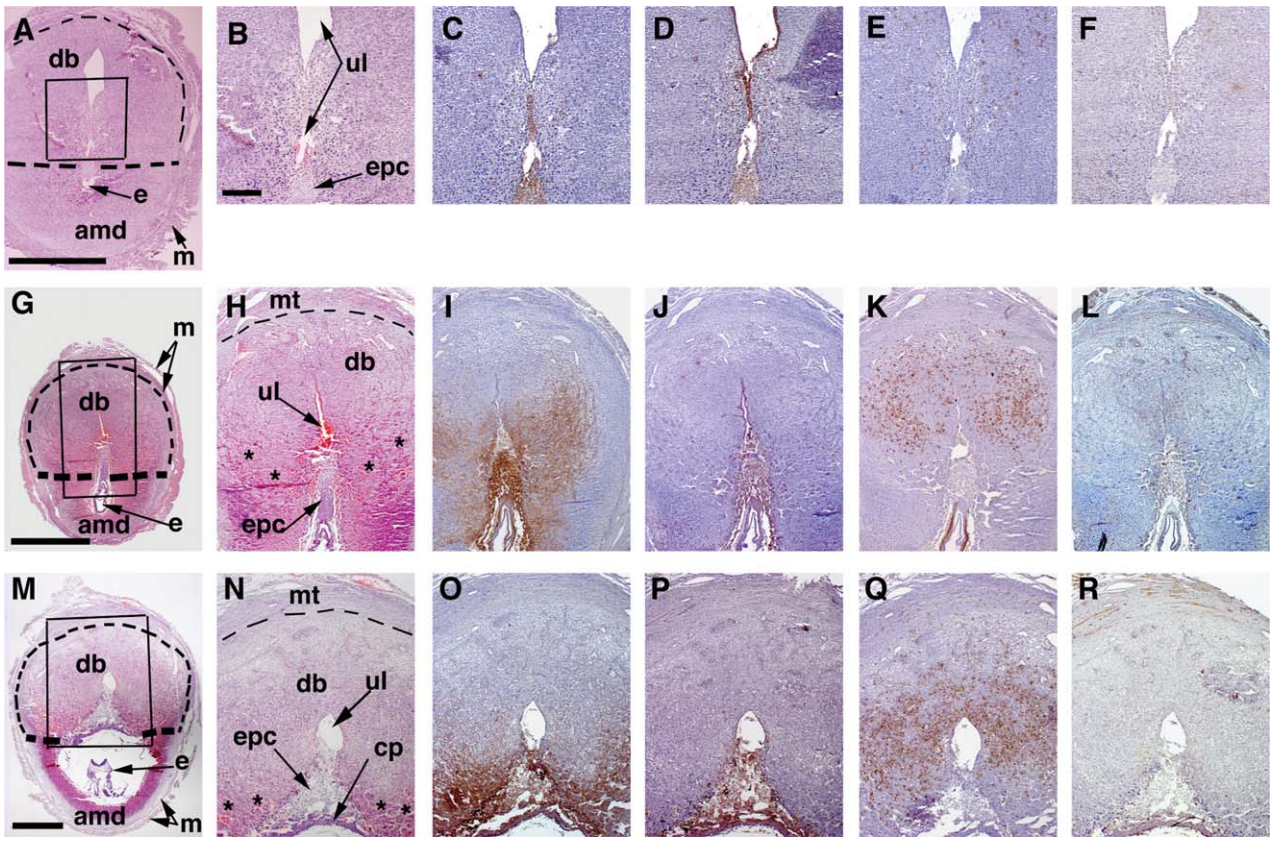

Fig. 5. Adjacent sections of the developing fetal placenta and decidua basalis at E6.5 (**A–F**), E7.5 (**G–L**) and E8.5 (**M–R**), stained with H/E (**A, B, G, H, M, N**), BS-I lectin (**C, I, O**), anti-cytokeratin antibody (**D, J, P**), DBA lectin (**E, K, Q**), and anti-ASMA antibody (**F, L, R**). In all images, the mesometrial pole is at the top of each panel. Panels B–F, H–L, and N–R are high magnification views of the areas enclosed by rectangles in A, G, and M, respectively. Note that BS-I lectin binding at E6.5 is restricted to the EPC and uterine lumen (ul) epithelium (C), but at E7.5 and E8.5 it is also found in the decidua basalis (I and O), in an area that is adjacent to the EPC that approximately encompasses the area occupied by the venous sinusoids (asterisks in H and N). Note that the chorionic plate (cp) is also BS-I positive (O). Panels A, H–L and N–R are of the same magnification; scale bar in A is 400 μm. Panels B-F are of the same magnification; scale bar in B is 200 μm. Scale bars in G and M are 1 mm. Amd: antimesometrial decidua; cp: chorionic plate; db: decidua basalis; e: embryo; epc: ectoplacental cone; m: myometrium; mt: mesometrial triangle; ul: uterine lumen remnant

uNK cell marker DBA lectin, in both the decidua basalis and the mesometrial triangle (Fig. 3G–J,Q,R,T,U). The absence of BS-I positivity in uNK cells at E6.5 (Fig. 3B,C), a stage when all uNKs are immature, but not later (i.e., when several uNK cell maturation stages coexist; Paffaro et al., 2003; Herington and Bany, 2007), suggested to us that BS-I binding may mark uNK cells of a specific maturation stage. To explore this, we examined the simultaneous localization of osteopontin and BS-I on the same section using double fluorescent immunohistochemistry from E8.5 onwards. Osteopontin (also referred to as SPP1) marks only the mature (granulated) uNK cells (Types II, III, and IV), but not the immature (Type I) ones (Paffaro et al., 2003; Herington and Bany, 2007). We show that BS-I lectin binding is confined to osteopontin-positive uNK cells in both the decidua basalis and the mesometrial triangle (Fig. 4 and data not shown). Interestingly, BS-I positivity was also present in the epithelium of uterine glands during the E6.5–E8.5 interval (Fig. 7A and data not shown) and in the perimetrium throughout the entire E6.5–E12.5 period (Fig. 7C and data not shown).

To obtain an estimate of the amount of available BS-I lectin binding sites within the various placental regions examined, we carried out a quantification analysis of the intensity of the chromogenic BS-I lectin signal at E7.5, E8.5, E10.5, and E12.5, using a previously reported methodology (Tolivia et al., 2006). At E7.5 and E8.5, a time when BS-1 lectin binding was detectable in all trophoblast cells, the following was found regarding the various trophoblast regions: (a) At E7.5 the strongest signal was that of pTG cells, whereas those in the EPC and chorionic trophoblast were not statistically different between them and collectively their signal strength was relatively weaker (about 37%–48% less). (b) At E8.5, the strongest signal was that of chorionic trophoblast and pTG cells (no statistical difference between them) whereas that of the EPC was about 25% less. (c) Between E7.5 and E8.5, there was no statistically significant change in the signal strength of pTG cells, but that of chorionic trophoblast increased by about 125% and that of the EPC by about 40% (Fig. 8). At E10.5, a stage when BS-I positivity was undetectable in pTG cells, BS-I signal strength in junctional zone trophoblast

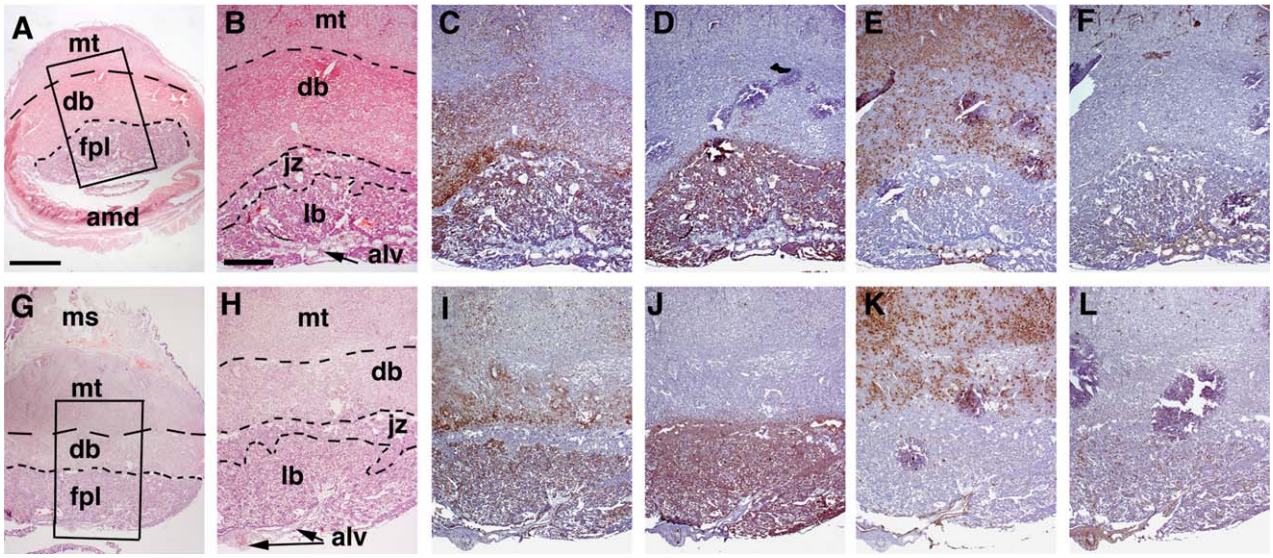

Fig. 6. Adjacent sections of the fetal placenta and decidua basalis at E10.5 (**A–F**) and E12.5 (**G–L**), stained with H/E (A, B, G, H), BS-I lectin (C, I), anti-cytokeratin antibody (D, J), DBA lectin (E, K) and anti-ASMA antibody (F, L). In all images, the mesometrial pole is at the top of each panel. Panels B–F and H–L are higher magnification views of the areas enclosed by rectangles in A and G, respectively. Note that at both stages, BS-I lectin binding is restricted to the decidua basalis and less so (appearing in scattered cells) in the mesometrial triangle, but it is absent from the allantoic vessels (alv) of the chorionic plate (C, I). Also note that in the fetal placenta BS-I positivity changes from E10.5 to E12.5, so that at E12.5 the junctional zone (jz) looses all signal and that in the labyrinth (lb) becomes reduced. Panels A and G are of the same magnification; scale bar in A is 1 mm. Panels B–F and H–L are of the same magnification; scale bar in B is 0.5 mm. Alv: allantoic vessels of the chorionic plate; amd: antimesometrial decidua; db: decidua basalis; fpl: fetal placenta; jz: junctional zone; lb: labyrinth; mt: mesometrial triangle

was the strongest, whilst that in labyrinthine trophoblast and labyrinthine fetal vasculature was weaker (about 20% and 30% less, respectively; Fig. 8). During the E10.5-to-E12.5 transition (when all trophoblast BS-I positivity was lost), the signal strength of labyrinthine fetal vasculature did not change in a statistically significant fashion (Fig. 8). Regarding BS-I lectin signal strength in the stroma of the decidua basalis we found the following: (a) Although BS-I positivity was undetectable in the mesometrial decidua basalis at E7.5 and E8.5, the signal strength in the antimesometrial edge of the decidua basalis increased between E7.5 and E8.5 by about 350%. (b) By E10.5 and E12.5, when this signal was detectable in both mesometrial and antimesometrial decidua basalis, that in the antimesometrial region was stronger (~50% stronger at E10.5 and about 260% stronger at E12.5). (c) During the E10.5-to-E12.5 period, the signal strength of the antimesometrial decidua basalis increased (by about 110%), whereas that of the mesometrial region did not show any statistically significant change (Fig. 8).

DISCUSSION

This study constitutes the first comprehensive description of the hitherto largely unexplored distribution of BS-I lectin binding during mouse placentation (E6.5–E12.5) by documenting the spatiotemporal presence of those oligosaccharide parts of glycoconjugates that bind this lectin (i.e., those with terminal DGalNAc or DGal) during this period. Our findings reveal that BS-I positivity is highly dynamic in both the fetal and maternal placenta, thereby contributing to the elucidation of the placental glycome during placentation. Moreover, this work establishes for the first time BS-I positivity as an early pan-trophoblast marker and a marker of the decidua basalis stroma of the venous sinusoid area during early placentation (E7.5–E8.5). In addition the results presented here establish BS-I lectin binding as a novel marker for a mature subset uNK cells throughout the entire period studied.

During placentation of the fetal placenta, our finding that BS-I lectin positivity during the E6.5–E7.5 period is present in the EPC, pTG cells, and primary trophoblast giant cells, is in accordance with previous work (Wu et al., 1983; Azuma et al., 1991; Tam et al., 1993). The stronger BS-I signal intensity of pTG cells relative to EPC cells at E7.5 and E8.5 indicates that these different trophoblast types also differ in their glycome profile (probably reflecting more BS-I binding sites in the former), suggesting that BS-I detected quantitative glycome differences may contribute to their cell type differences. Moreover, the increases in BS-I lectin signal strength in EPC and chorionic trophoblast, but not in pTG cells, during the E7.5-to-E8.5 period suggest the involvement of glycans that bind this lectin in changes that normally take place within the EPC and chorion during this period (Simmons et al., 2008b). Our novel finding that BS-I lectin binding marks labyrinthine and junctional zone trophoblast at E10.5/E11.5 as well as their progenitors (the E7.5/E8.5 EPC and chorion/chorionic plate trophoblast) suggests that glycoconjugates that bind this lectin are involved in the differentiation of these trophoblast types. The difference in BS-I lectin positivity strength between junctional zone and labyrinthine trophoblasts at E10.5 shows a difference in their glycan profile that

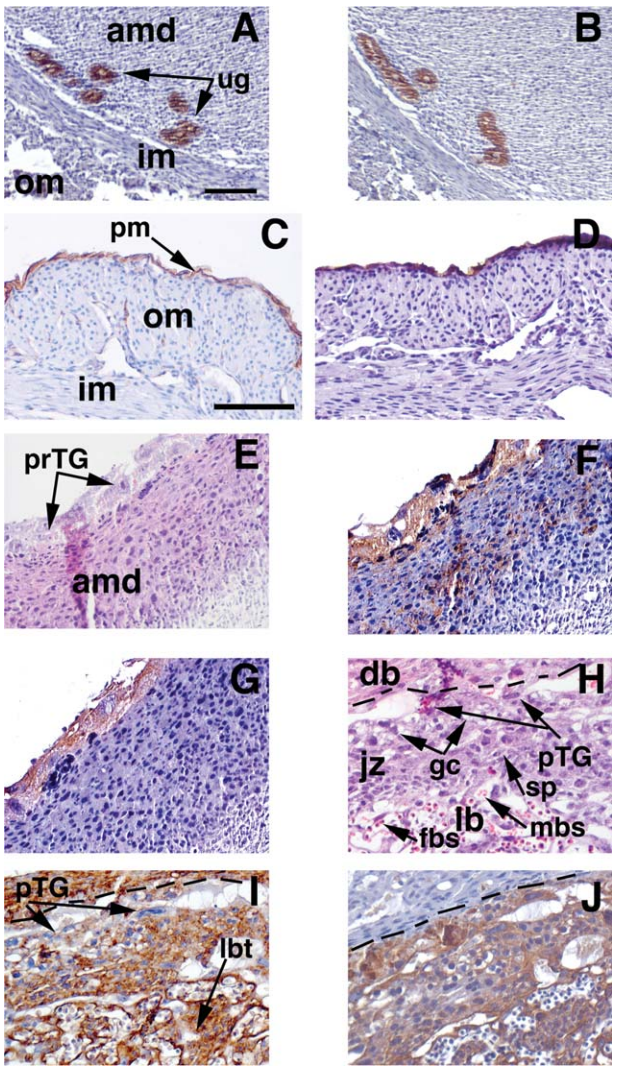

Fig. 7. Adjacent sections of various areas of the fetal placenta and uterus at E6.5 (**A, B**), E7.5 (**C, D**), E8.5 (**E–G**), and E11.5 (**H–J**) stained with BS-I lectin (A, C, F, I), H/E (E, H), and an anti-cytokeratin antibody (B, D, G, J). Panels A, C, and F show BS-I positivity in the epithelium of uterine glands (ug), the perimetrium and the primary trophoblast giant (prTG) cells, respectively. All these are marked by cytokeratin positivity (B, D, G). Panel I shows BS-I binding to all trophoblasts of the fetal placenta except the pTG cells. Panels A, B, and E–G are of the same magnification; scale bar in A is 100 μm. Panels C, D, and H–J are of the same magnification; scale bar in A is 100 μm. Amd: antimesometrial decidua; db: decidua basalis; fbs: fetal blood spaces of the labyrinth; gc: glycogen trophoblast cells; im: inner myometrium; jz: junctional zone; lb: labyrinth; lbt: labyrinthine trophoblast; mbs: maternal blood spaces of the labyrinth; om: outer myometrium; pm: perimetrium; pTG: parietal trophoblast giant cells; prTG: primary trophoblast giant cells; sp: spongiotrophoblast; ug: uterine gland

may reflect the functional and/or gene expression differences that exist between them (Georgiades et al., 2002). The subsequent loss of positivity for this lectin from all fetal trophoblasts by E12.5 indicates that BS-I binding glycoconjugates may also regulate a trophoblast maturation switch that takes place between E10.5/11.5 and E12.5, but not later. An example of such a maturation switch during this period is the previously documented loss of *Prl3d1* (previously known as *Pl1*) expression from pTG cells and the onset of expression of the *Prl8a8* and *Prl2a1* genes in spongiotrophoblasts and trophoblast glycogen cells of the junctional zone, respectively (Simmons et al., 2008a). Our results agree with those of a previous study (Detmar et al., 2008) regarding BS-I lectin being a marker of labyrinthine fetal capillary endothelium. Importantly, our findings extend these results in that we found that this situation exists from as early as E10.5 and that the strength of BS-I positivity in this does not change during the E10.5-to-E12.5 period.

Within the maternal placenta (decidua basalis) at E7.5 and E8.5, BS-I lectin binding is shown for the first time to mark the decidual stroma of the venous sinusoids next to the EPC (i.e., the antimesometrial region of the decidua basalis). This probably marks decidual stroma cells that are more differentiated than the rest, as judged by their stronger eosinophilic reaction (upon H/E staining of adjacent sections) and their closeness to the conceptus (Davies and Glasser, 1968; Stewart and Peel, 1979). Interestingly, the increase in BS-I lectin signal intensity in the antimesometrial decidua basalis between E7.5 and E8.5 suggests that an increase in BS-I lectin binding sites may contribute to the progression of decidualization in this part of the decidua basalis during this period (Abrahamsohn and Zorn, 1993). Subsequently, by E10.5, this positivity was found to also expand to the stroma of the mesometrial decidua basalis, thereby marking the entire decidua basalis, but not to that of the mesometrial triangle. This makes BS-I lectin positivity a novel tool for distinguishing between the stroma of the decidua basalis and that of the mesometrial triangle at least during the period from E10.5 to E12.5. Our detection of BS-I binding to the endothelium of the spiral arteries at E7.5, but not earlier or later, may be related to the acquisition of muscular wall by them, an event that normally takes place between E6.5 and E7.5 (Elia et al., 2011). This study also establishes BS-I lectin binding as a novel marker of mature uNK cells, as shown by the colocalization of BS-I lectin binding and osteopontin positivity in these cells. Mature uNK cells, unlike their immature counterparts, are thought to be involved in decidual spiral artery wall modification, an important event of placentation (Charalambous et al., 2012). This pattern of BS-I positivity in uNKs (i.e., absence from immature and presence in mature uNK cells) implicates the involvement of changes in the glycome (and specifically those detected by BS-I lectin) in the poorly understood phenomenon of uNK cell maturation.

It must be noted that absence of, or differences in, the strength of BS-I lectin positivity can be attributed to either (a) absence of or quantitative differences in the amount of BS-I binding glycans, or (b) "masking" or "unmasking" of these glycans by sialic acid. This is because sialic acids, a family of nine-carbon acidic sugars that are negatively charged, were shown to bind glycans, including those that are the targets of BS-I lectin, thereby making them unavailable (or more available in the case of sialic acid loss) for lectin binding (Schauer, 1985; Jowett et al., 1994). Nevertheless, this work shows spatio-temporal differences in available BS-I binding sites during placentation, irrespective of whether this is due to differences in their actual amounts or due to their masking (or unmasking) by sialic acid.

Embryonic Stage	BS-I lectin signal intensity							
	EPC trophoblast Mean +/-SEM (n)	Chorionic trophoblast Mean +/-SEM (n)	Parietal trophoblast giant (pTG) cells Mean +/-SEM (n)	Junctional zone trophoblast Mean +/-SEM (n)	Labyrinthine trophoblast Mean +/-SEM (n)	Labyrinthine fetal vasculature Mean +/-SEM (n)	Decidua basalis (anti-mesometrial end) Mean +/-SEM (n)	Decidua basalis (mesometrial region) Mean +/-SEM (n)
E7.5	0.18* a +/-0.01 (n=12)	0.15* a +/-0.02 (n=12)	0.29 b +/- 0.02 (n=15)	NA	NA	NA	0.08* c +/-0.01 (n=15)	0
E8.5	0.25 a +/- 0.02 (n=14)	0.33 b +/- 0.02 (n=25)	0.34 b +/-0.02 (n=21)	NA	NA	NA	0.36* b +/- 0.02 (n=20)	0
E10.5	NA	NA	0	0.31 a +/- 0.01 (n=20)	0.25 b +/- 0.02 (n=19)	0.21 c +/- 0.02 (n=15)	0.17* d +/- 0.01 (n=18)	0.11 e +/- 0.01 n=15
E12.5	NA	NA	0	0	0	0.22 a +/- 0.02 (n=21)	0.35 b +/- 0.02 (n=19)	0.10 c +/- 0.01 (n=22)

Fig. 8. BS-I lectin signal intensity within various placental compartments at E7.5, E8.5, E10.5, and E12.5. Values shown are the means of the "mean gray values" of each placental region measured: Absence of BS-I positivity has a zero value and maximum BS-I signal strength has a value of one (see "Materials and Methods" section for more details). Within each stage, different superscript letters denote statistically significant differences in BS-I signal intensities between different placental regions, using the "One-way ANOVA" test ($P < 0.05$). Any value with a superscript asterisk denotes a statistical difference between it and the value of the same placental compartment at the next embryonic stage, based on the "two-tailed unpaired Student's t-test" ($P < 0.05$). pTG cells at E7.5 and E8.5 were defined as the peripheral region of the EPC. Zero values denote regions without any BS-I positivity above background. EPC: ectoplacental cone; NA: nonapplicable; SEM: standard error of the mean; n: number of randomly chosen areas within a given placental compartment whose BS-I signal intensity was measured

Our findings may be clinically relevant because (a) they show similarities with the spatio-temporal pattern of BS-I lectin binding during human placentation and (b) BS-I binding patterns are altered in early human placental pathology. Specifically, our detection of BS-I positivity in the vasculature of the fetal placenta as well as in the fetal placental trophoblast (e.g., labyrinthine trophoblast) during placentation but not in the mature placenta (E12.5), is in agreement with human work. BS-I binding was reported in fetal placental vasculature throughout human gestation and in human fetal placenta trophoblast (villous trophoblast) during the first trimester (i.e., during placentation), but not in the mature placenta (either during the second trimester or at term; Foidart et al., 1990; Thrower et al., 1991). Moreover, in molar pregnancies (where the placenta fails to form properly and trophoblast tissue is abnormal) BS-I binding patterns in villous trophoblast were reported to be abnormal (Thrower et al., 1991).

Taken together, the findings of this work extend knowledge regarding the dynamic nature of the glycome during mouse placentation. They provide the first detailed description of BS-I lectin binding patterns during mouse placentation and implicate the glycans that bind this lectin in important placentation events such as the differentiation of junctional zone and labyrinthine trophoblasts from their precursors and the maturation of pTG cells and uNK cells. In addition, this work establishes this lectin as a pan-trophoblast marker during early placentation and as a marker of mature uNK cells.

ACKNOWLEDGEMENTS

The authors thank the University of Cyprus for funding and all members of the Georgiades laboratory for technical assistance and mouse husbandry.

LITERATURE CITED

Abrahamsohn PA, Zorn TM. 1993. Implantation and decidualization in rodents. J Exp Zool 266:603–628.

Ain R, Canham LN, Soares MJ. 2003. Gestation stage-dependent intrauterine trophoblast cell invasion in the rat and mouse: novel endocrine phenotype and regulation. Dev Biol 260:176–190.

Ambrosi M, Cameron NR, Davis BG. 2005. Lectins: tools for the molecular understanding of the glycocode. Org Biomol Chem 3: 1593–1608.

Azuma M, Kanai Y, Ogura A, Kurohmaru M, Hayashi Y. 1991. Changes in cell surface and intracellular glycoproteins of trophoblastic giant cells during mouse placentation. Histochemistry 95:541–548.

Charalambous F, Elia A, Georgiades P. 2012. Decidual spiral artery remodeling during early post-implantation period in mice: investigation of associations with decidual uNK cells and invasive trophoblast. Biochem Biophys Res Commun 417:847–852.

Cross JC, Nakano H, Natale DR, Simmons DG, Watson ED. 2006. Branching morphogenesis during development of placental villi. Differentiation 74:393–401.

Davies J, Glasser SR. 1968. Histological and fine structural observations on the placenta of the rat. Acta Anat (Basel) 69:542–608.

Detmar J, Rennie MY, Whiteley KJ, Qu D, Taniuchi Y, Shang X, Casper RF, Adamson SL, Sled JG, Jurisicova A. 2008. Fetal growth restriction triggered by polycyclic aromatic hydrocarbons is associated with altered placental vasculature and AhR-dependent changes in cell death. Am J Physiol Endocrinol Metab 295:E519–E530.

Elia A, Charalambous F, Georgiades P. 2011. New phenotypic aspects of the decidual spiral artery wall during early post-implantation mouse pregnancy. Biochem Biophys Res Commun 416:211–216.

Foidart JM, Christiane Y, Emonard H. 1990. Interactions between the human trophoblast cells and the extraeellular matrix of the endometrium. Specific expression of a-galactose residues by invasive human trophoblastic cells. Trophoblast Res 4:159–177.

Freeze HH, Elbein AD. 2009. Glycosylation Precursors. In: Varki A, Cummings RD, Esko JD, editors. Essentials of Glycobiology. 2nd ed. New York: Cold Spring Harbor Press. p 47–62.

Gabius HJ, Wu AM. 2006. The emerging functionality of endogenous lectins: a primer to the concept and a case study on galectins including medical implications. Chang Gung Med J 29:37–62.

Georgiades P, Ferguson-Smith AC, Burton GJ. 2002 Comparative developmental anatomy of the murine and human definitive placentae. Placenta 23:3–19.

Herington JL, Bany BM. 2007. The conceptus increases secreted phosphoprotein 1 gene expression in the mouse uterus during the progression of decidualization mainly due to its effects on uterine natural killer cells. Reproduction 133:1213–1221.

Hu D, Cross JC. 2010. Development and function of trophoblast giant cells in the rodent placenta. Int J Dev Biol 54:341–354.

Ito F, Chou JY. 1984. Suppression of placental alkaline phosphatase biosynthesis by tunicamycin. J Biol Chem 259:14997–14999.

Jowett AK, Kimber SJ, Ferguson MW. 1994. Sialylation of terminal saccharides of glycoconjugates expressed by murine molar tooth germs developing in vitro and in vivo. J Anat 185:85.

Laitinen L. 1987. Griffonia simplicifolia lectins bind specifically to endothelial cells and some epithelial cells in mouse tissues. Histochem J 19:225–234.

Laughlin ST, Bertozzi CR. 2009. Imaging the glycome. Proc Natl Acad Sci USA 106:12–17.

Lescar J, Loris R, Mitchell E, Gautier C, Chazalet V, Cox V, Wyns L, Pérez S, Breton C, Imberty A. 2002. Isolectins I-A and I-B of Griffonia (Bandeiraea) simplicifolia. Crystal structure of metal-free GS I-B(4) and molecular basis for metal binding and monosaccharide specificity. J Biol Chem 277:6608–6614.

Marini M, Bonaccini L, Thyrion GDZ, Vichi D, Parretti E, Sgambati E. 2011. Distribution of sugar residues in human placentas from pregnancies complicated by hypertensive disorders. Acta Histochem 113:815–825.

Muthana SM, Campbell CT, Gildersleeve JC. 2012. Modifications of glycans: biological significance and therapeutic opportunities. ACS Chem Biol 7:31–43.

Ohtsubo K, Marth JD. 2006. Glycosylation in cellular mechanisms of health and disease. Cell 126:855–867.

Paffaro VA, Jr., Bizinotto MC, Joazeiro PP, Yamada AT. 2003. Subset classification of mouse uterine natural killer cells by DBA lectin reactivity. Placenta 24:479–488.

Rüdiger H, Gabius HJ. 2001. Plant lectins: occurrence, biochemistry, functions and applications. Glycoconj J 18:589–613.

Schauer, R. 1985. Sialic acids and their role as biological masks. Trend Biochem Sci 10:357–360.

Šerman L, Šerman A, Lauc G, Milić A, Latin V, Aleksandrova A, Šerman D. 2004. Comparison of glycosylation patterns of placental proteins between normal pregnancy and missed abortion. Coll Antropol 28:301–308.

Simmons DG, Natale DR, Begay V, Hughes M, Leutz A, Cross JC. 2008b. Early patterning of the chorion leads to the trilaminar trophoblast cell structure in the placental labyrinth. Development 135:2083–2091.

Simmons DG, Rawn S, Davies A, Hughes M, Cross JC. 2008a. Spatial and temporal expression of the 23 murine Prolactin/Placental Lactogen-related genes is not associated with their position in the locus. BMC Genomics 9:352.

Stewart I, Peel S. 1979. The differentiation of the decidua and the distribution of metrial gland cells in the pregnant mouse uterus. Cell Tissue Res 187:167–179.

Tam PP, Williams EA, Chan WY. 1993. Gastrulation in the mouse embryo: ultrastructural and molecular aspects of germ layer morphogenesis. Microsc Res Tech 26:301–328.

Than NG, Romero R, Kim CJ, McGowen MR, Papp Z, Wildman DE. 2012. Galectins: guardians of eutherian pregnancy at the maternal-fetal interface. Trend Endocrinol Metab 23:23–31.

Thrower S, Bulmer JN, Griffin NR, Wells M. 1991. Further studies of lectin binding by villous and extravillous trophoblast in normal and pathological pregnancy. Int J Gynecol Pathol 10:238–251.

Tolivia J, Navarro A, del Valle E, Perez C, Ordoñez C, Martínez E. 2006. Application of Photoshop and Scion Image analysis to quantification of signals in histochemistry, immunocytochemistry and hybridocytochemistry. Anal Quant Cytol Histol 28:43–53.

Varki A, Etzler ME, Cummings RD, Esko JD. 2009. Discovery and Classification of Glycan-Binding Proteins. In: Varki A, Cummings RD, Esko JD, editors. Essentials of Glycobiology. 2nd ed. New York: Cold Spring Harbor Press. p 375–386.

Varki A, Sharon N. 2009. Historical Background and Overview. In: Varki A, Cummings RD, Esko JD, editors. Essentials of Glycobiology. 2nd ed. New York: Cold Spring Harbor Press. p 1–22.

Webb CG, Duksin D. 1981. Involvement of glycoproteins in the development of early mouse embryos: effect of tunicamycin and alpha, alpha' dipyridyl in vitro. Differentiation 20:81–86.

Wood C, Kabat EA, Murphy LA, Goldstein IJ. 1979. Immunochemical studies of the combining sites of the two isolectins, A4 and B4, isolated from Bandeiraea simplicifolia. Arch Biochem Biophys 198:1–11.

Wu TC, Wan YJ, Damjanov I. 1983. Fluorescein-conjugated Bandeiraea simplicifolia lectin as a marker of endodermal, yolk sac, and trophoblastic differentiation in the mouse embryo. Differentiation 24:55–59.

Zhang J, Chen Z, Smith GN, Croy BA. 2011. Natural killer cell-triggered vascular transformation: maternal care before birth? Cell Mol Immunol 8:1–11.